International Journal of Heat and Mass Transfer 54 (2011) 894–909

Contents lists available at ScienceDirect

International Journal of Heat and Mass Transfer

journal homepage: www.elsevier.com/locate/ijhmt

Control of mixed convection in lid-driven enclosures using conductive triangular fins

Changzheng Sun [a], Bo Yu [a,*], Hakan F. Oztop [b,*,1], Yi Wang [a], Jinjia Wei [c]

[a] *Beijing Key Laboratory of Urban Oil and Gas Distribution Technology, China University of Petroleum-Beijing, Beijing 102249, PR China*
[b] *Department of Mechanical Education, Firat University, TR-23119 Elazig, Turkey*
[c] *State Key Lab. of Multiphase Flow in Power Engineering, Xi'an Jiaotong University, Xi'an, China*

ARTICLE INFO

Article history:
Received 29 June 2009
Received in revised form 24 September 2010
Accepted 28 September 2010
Available online 26 November 2010

Keywords:
Mixed convection
Lid-driven cavity
Triangular fin

ABSTRACT

Control of mixed convection (combined forced and natural convection) in a lid-driven square cavity is performed using a short triangular conductive fin. A numerical technique is used to simulate the flow and temperature fields. The vertical walls of the cavity are differentially heated. Both the top lid and the bottom wall are adiabatic. The fin is located on one of the motionless walls of the cavity. Three different cases have been studied based on the location of the fin. In this context, Cases I, II and III refer to the fin on the left, bottom and right walls, respectively. Results are presented for $+x$ and $-x$ directions of the top lid in horizontal axis and different Richardson numbers as $Ri = 0.1$, 1.0 and 10.0. It is observed that the triangular fin is a good control parameter for heat transfer, temperature distribution and flow field.

1. Introduction

Lid-driven flow in a cavity has been an important research subject due to its wide spectrum of engineering applications. These applications can be traced to oil extraction, cooling of electronic equipments, design of heat exchangers, flow and heat transfer in solar ponds, crystal growth, dynamics of lakes and float glass productions [1–3]. Earlier studies on lid-driven cavities can be mainly classified into three groups as (a) cavity flows generated by double sided moving lids in the absence of buoyancy effects, (b) cavity flows including buoyancy effects, namely mixed convection, for double sided or single moving lid and (c) cavity flows with fin attached to the wall to control heat transfer. The problem of lid-driven cavity flow is also a benchmark configuration for the evaluation of numerical solution procedures for the Navier–Stokes equations [4–7].

Lid-driven cavities with vertical moving lids were studied by Chamkha [8] including hydromagnetic mixed convection with internal heat generation or absorption. Aydin [9] compared aiding and opposing mechanism in a shear-driven and buoyancy-driven cavity. Freitas et al. [10] and Iwatsu and Hyun [11] studied the three dimensional lid-driven cavity flows. Sharif [12], Morzynski and Popiel [13], Freitas and Street [14], Iwatsu et al. [15], and Mohamad and Viskanta [16] made numerical analyses on effects of horizontally moving lid in cavities. All of these authors indicated that the ratio of lid velocity to power of buoyancy force was the most important parameter to flow field, temperature distribution and heat transfer. The pioneer works on mixed convection in double sided lid-driven cavities were published by Oztop and Dagtekin [17] and Alleborn et al. [18]. They indicated that moving direction of lid was extremely important to mixed convection.

Control of heat transfer and fluid flow in a lid-driven cavity is an important issue to save energy and enhance the total quality of thermal system. Unfortunately, numbers of studies on this phenomenon are extremely limited in earlier literature. In this context, Shi and Khodadadi [19–21] indicated that the flow and heat transfer can be controlled using an oscillating fin attached on the motionless wall through a numerical study. Oztop [22] made a study to control heat and fluid flow with an adiabatic rectangular body. Dagtekin and Oztop [23] modeled the cooling of electronic devices in a lid-driven enclosure. Mahapatra et al. [24] solved the mixed convection problem in differentially heated square enclosure with two adiabatic partitions (ceiling and floor) using FLUENT commercial software. They indicated that the effect of the partition location on heat transfer is marginal for $Ri = 1.0$ and more pronounced for $Ri = 0.1$. Mansutti et al. [25] applied a discrete vector potential model to unsteady incompressible viscous flow using a lid-driven cavity with a square body insertion. As shown in the literature survey [26–33], there are very few studies on mixed convection heat transfer in lid-driven cavities.

The main aim of the present study is to examine the control parameters of mixed convection in a top lid using triangular cross-sectional conductive fin. To examine heat transfer by the

* Corresponding authors. Tel.: +86 1089733849 (B. Yu), Tel.: +90 424 237 0000x4356; fax: +90 424 241 5526 (H.F. Oztop).
E-mail addresses: yubobox@cup.edu.cn (B. Yu), hfoztop1@gmail.com, hfoztop1@yahoo.com (H.F. Oztop).
[1] Visiting Professor, King Saud University, Department of Mechanical Engineering, Riyadh, Saudi Arabia.

0017-9310/$ - see front matter
doi:10.1016/j.ijheatmasstransfer.2010.09.068

Nomenclature

A	aspect ratio, H/L
C_p	specific heat, kJ/(kg K)
D	diameter, m
Gr	Grashof number (=$g\beta(T_h - T_c)L^3/\nu^2$)
H	height of the cavity, m
K	thermal conductivity ratio (=λ_f/λ_s)
L	length of the cavity, m
n	any direction
Nu	Nusselt number
p	pressure, Pa
Pr	Prandtl number (=ν/α)
Re	Reynolds number (=uH/ν)
Ri	Richardson number (=Gr/Re^2)
Ra	Rayleigh number (=$PrGr$)
T	temperature, K
u, v	velocities, m/s
x, y	coordinates, m

Greek symbols

α	thermal diffusivity, m^2/s
β	thermal expansion coefficient, K^{-1}
θ	dimensionless temperature (=$(T - T_c)/(T_h - T_c)$)
λ	thermal conductivity, W/(m K)
ν	kinematic viscosity, m^2/s
ρ	density, kg/m^3

Subscripts

c	cold
f	fluid
h	hot
p	top lid
s	solid
w	wall
$cond$	conduction

fin, three locations of the fin were tested. These cases were also compared with the case of the lid-driven cavity without insertion. The detailed analyses of heat transfer and fluid flow were carried out using control volume method.

2. Physical model

Sketch of the considered physical model is given in Fig. 1(a)–(d) for four different cases in this study. Fig. 1(a) depicts Case 0 without triangular fin inside the cavity. Fig. 1(b) describes Case I in which the triangular fin is attached to the left wall. Fig. 1(c) shows Case II in which the triangular fin is attached to the bottom wall. Fig. 1(d) is Case III in which the triangular fin is attached to the right wall. The fin is isosceles triangular. Horizontal walls are kept as adiabatic. The top lid of the cavity moves in two different ways as $+x$ or $-x$ direction with constant velocity. Vertical walls are differentially heated and isothermal while the left wall has higher temperature than the right wall.

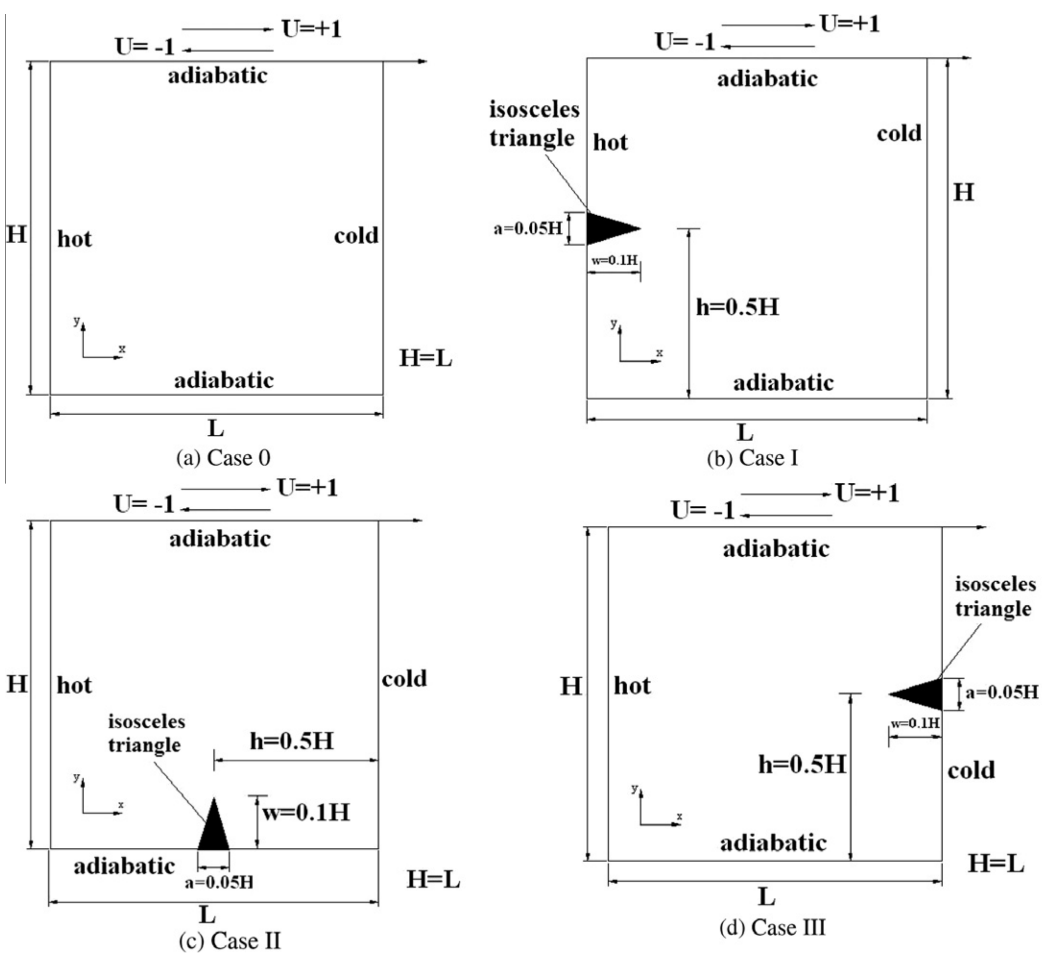

Fig. 1. Configurations for studied cases.

Gravity acts are considered in $-y$ direction. Fig. 2 illustrates the detailed view for an example configuration with dimensions and coordinates. The cavity is square ($H = L$). The distance of the triangle top to the cavity bottom is $h = 0.5H$. The height of the triangle is $w = 0.1H$ and the bottom length of the triangle is $a = 0.05H$.

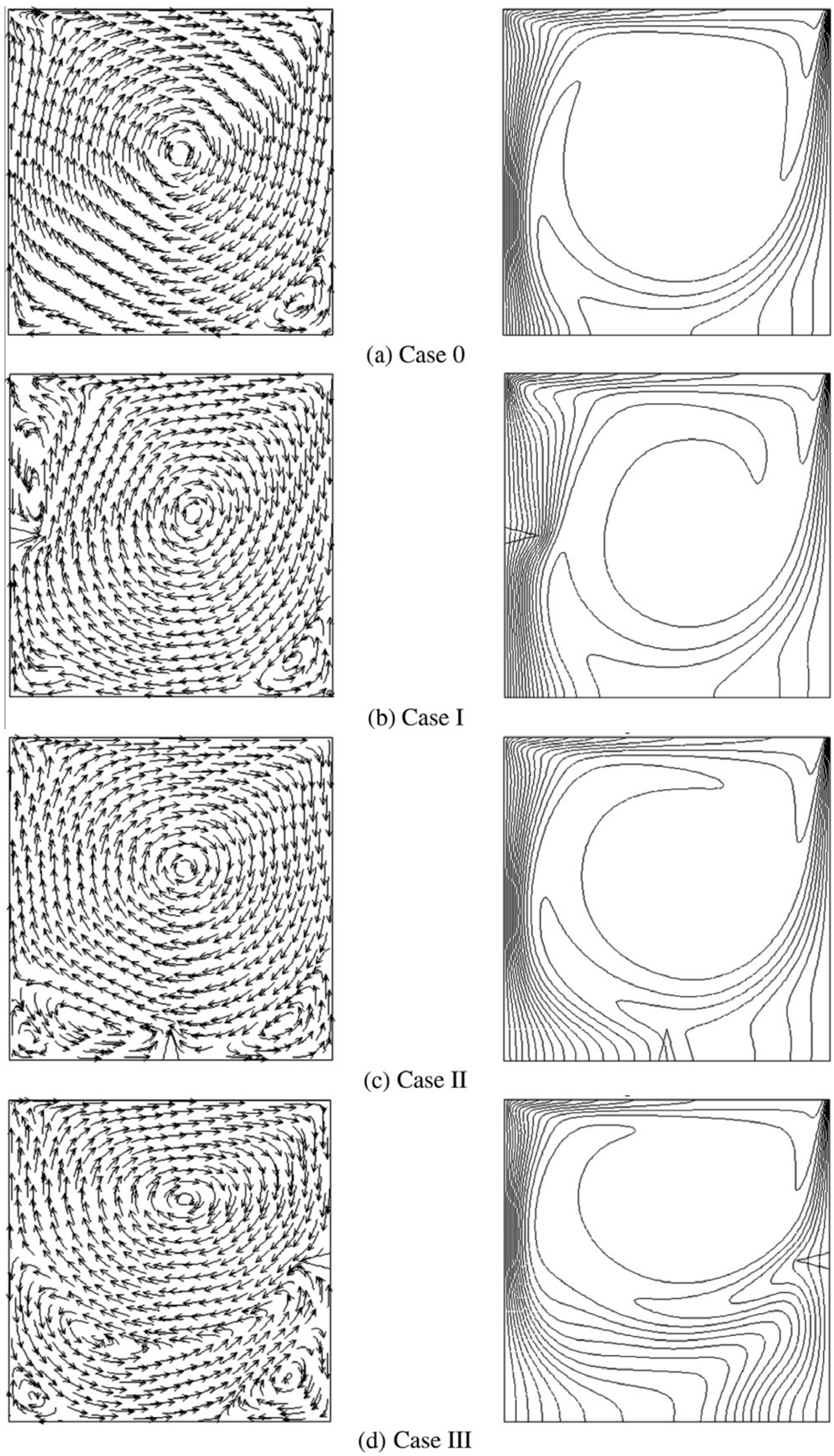

Fig. 2. Streamlines with arrows and isotherms for different cases with lid moving in the +x direction at $Ri = 0.1$.

Table 1
Comparison with Refs. [35–38] at $Ra = 10^4$ and $Ra = 10^5$.

	Present work		Barakos et al. [35]		Markatos and Pericleous [36]		De Vahl Davis [37]		Fusegi et al. [38]	
	$Ra = 10^4$	$Ra = 10^5$	$Ra = 10^4$	$Ra = 10^5$	$Ra = 10^4$	$Ra = 10^5$	$Ra = 10^4$	$Ra = 10^5$	$Ra = 10^4$	$Ra = 10^5$
Case 0										
$\overline{Nu}$	2.29	4.61	2.25	4.51	2.20	4.43	2.24	4.52	2.30	4.65
$Nu_{\max}$	3.60	7.94	3.54	7.64	3.48	7.63	3.53	7.72	3.65	7.80
$Nu_{\min}$	0.59	0.73	0.58	0.77	0.64	0.82	0.59	0.73	0.61	0.79

Table 2
Mean Nusselt numbers at $Gr=10^5$ for different Ri and K.

	$U = -1$			$U = +1$		
	$Ri = 0.1$	$Ri = 1.0$	$Ri = 10.0$	$Ri = 0.1$	$Ri = 1.0$	$Ri = 10.0$
Case I						
$K = 0.1$	6.22	4.82	3.74	5.70	4.68	4.21
$K = 1.0$	6.16	4.75	3.64	5.50	4.57	4.12
$K = 10.0$	6.15	4.72	3.61	5.45	4.55	4.09
Case II						
$K = 0.1$	6.43	4.92	3.94	6.81	5.06	4.50
$K = 1.0$	6.42	4.92	3.94	6.81	5.06	4.50
$K = 10.0$	6.42	4.92	3.94	6.80	5.06	4.50
Case III						
$K = 0.1$	5.36	4.49	3.69	6.57	4.92	4.27
$K = 1.0$	5.18	4.38	3.58	6.47	4.83	4.18
$K = 10.0$	5.09	4.36	3.56	6.44	4.80	4.15

3. Governing equations and boundary conditions

The study domain is two-dimensional cavity with a moving lid and a solid triangular fin. Fluid inside the cavity is considered as Newtonian, incompressible and constant properties. The flow is laminar and steady-state. Boussinesq approximation is performed, i.e., all physical properties of the fluid except density in the buoyant force term are constant. In these conditions, the continuity, momentum and energy equations can be written as follows:

$$\frac{\partial u}{\partial x}+\frac{\partial v}{\partial y}=0 \tag{1}$$

$$u\frac{\partial u}{\partial x}+v\frac{\partial u}{\partial y}=-\frac{1}{\rho}\frac{\partial p}{\partial x}+\nu\left(\frac{\partial^2 u}{\partial x^2}+\frac{\partial^2 u}{\partial y^2}\right) \tag{2}$$

$$u\frac{\partial v}{\partial x}+v\frac{\partial v}{\partial y}=-\frac{1}{\rho}\frac{\partial p}{\partial y}+\nu\left(\frac{\partial^2 v}{\partial x^2}+\frac{\partial^2 v}{\partial y^2}\right)+g\beta(T-T_c) \tag{3}$$

$$u\frac{\partial T}{\partial x}+v\frac{\partial T}{\partial y}=\frac{\lambda}{\rho C_p}\left(\frac{\partial^2 T}{\partial x^2}+\frac{\partial^2 T}{\partial y^2}\right) \tag{4}$$

Heat conduction equation is valid on the fin:

$$\frac{\partial^2 T}{\partial x^2}+\frac{\partial^2 T}{\partial y^2}=0 \tag{5}$$

The following non-dimensional variables are defined as:

$$\theta=\frac{T-T_c}{T_h-T_c},\quad Re=\frac{uH}{\nu},\quad Gr=\frac{g\beta(T_h-T_c)H^3}{\nu^2},\quad Pr=\frac{\nu}{\alpha},\quad K=\frac{\lambda_f}{\lambda_s}$$
$$X=\frac{x}{H},\quad Y=\frac{y}{H},\quad U=\frac{u}{u_P},\quad V=\frac{v}{u_P},\quad P=\frac{p}{\rho u_P^2} \tag{6}$$

where θ is dimensionless temperature, Re is Reynolds number, Gr is Grashof number, Pr is Prandtl number and K is thermal conductivity ratio. Richardson number is defined by Eq. (7). It characterizes the mixed convection flow where Gr and Re represent the strength of the natural and forced convection effects, respectively. For $Ri \to 0$, the heat transfer regime is forced convection and $Ri \to \infty$, natural convection

$$Ri=\frac{Gr}{Re^2} \tag{7}$$

Using the above parameters, the governing equations (1)–(4) can be written in dimensionless forms as:

$$\frac{\partial U}{\partial X}+\frac{\partial V}{\partial Y}=0 \tag{8}$$

$$U\frac{\partial U}{\partial X}+V\frac{\partial U}{\partial Y}=-\frac{\partial P}{\partial X}+\frac{1}{Re}\left(\frac{\partial^2 U}{\partial X^2}+\frac{\partial^2 U}{\partial Y^2}\right) \tag{9}$$

$$U\frac{\partial V}{\partial X}+V\frac{\partial V}{\partial Y}=-\frac{\partial P}{\partial Y}+\frac{1}{Re}\left(\frac{\partial^2 V}{\partial X^2}+\frac{\partial^2 V}{\partial Y^2}\right)+Ri\theta \tag{10}$$

$$U\frac{\partial \theta}{\partial X}+V\frac{\partial \theta}{\partial Y}=\frac{1}{RePr}\left(\frac{\partial^2 \theta}{\partial X^2}+\frac{\partial^2 \theta}{\partial Y^2}\right) \tag{11}$$

Heat conduction equation of solid fin is given as:

$$\frac{\partial^2 \theta}{\partial X^2}+\frac{\partial^2 \theta}{\partial Y^2}=0 \tag{12}$$

Local Nusselt number is:

$$Nu_y=\frac{(\partial\theta/\partial X)_w}{(\partial\theta/\partial X)_{cond}} \tag{13}$$

Note that $(\partial\theta/\partial X)_{cond}$ is the temperature gradient for conductive heat transfer without a partition. The average Nusselt number is calculated by integrating the local Nusselt number along the wall as follows:

Table 3
Mean Nusselt numbers and reduction at $Gr = 10^5$ and $K = 1.0$.

	$U = -1$						$U = +1$					
	$Ri = 0.1$	σ (%)	$Ri = 1.0$	σ (%)	$Ri = 10.0$	σ (%)	$Ri = 0.1$	σ (%)	$Ri = 1.0$	σ (%)	$Ri = 10.0$	σ (%)
Case 0	6.75	–	5.01	–	4.01	–	7.46	–	5.29	–	4.61	–
Case I	6.16	8.74	4.75	5.19	3.64	9.23	5.50	26.27	4.57	13.61	4.12	10.63
Case II	6.42	4.89	4.92	1.8	3.94	1.75	6.81	8.71	5.06	4.35	4.50	2.39
Case III	5.18	23.26	4.38	12.57	3.58	10.72	6.47	13.27	4.83	8.70	4.18	9.33

$\sigma=\frac{\overline{Nu}_{\mathrm{Case0}}-\overline{Nu}_{\mathrm{Case}(J)}}{\overline{Nu}_{\mathrm{Case0}}}\times 100\% \quad J=\mathrm{I,II,III}.$

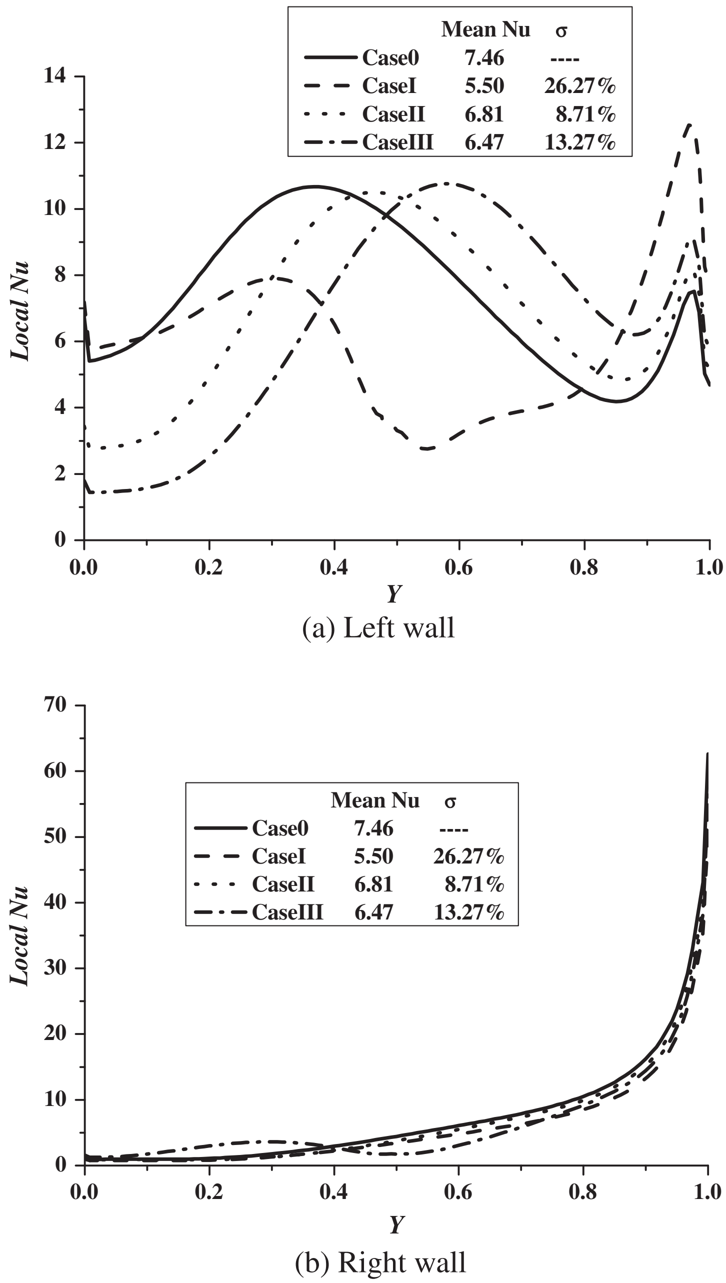

Fig. 3. Local Nusselt number and the mean *Nu* for different cases with lid moving in the +*x* direction at *Ri* = 0.1. $^*\sigma = \frac{\overline{Nu}_{\mathrm{Case0}} - \overline{Nu}_{\mathrm{Case}(J)}}{\overline{Nu}_{\mathrm{Case0}}} \times 100\% \quad J = \mathrm{I, II, III}$.

$$\overline{Nu} = \int_0^1 Nu_y \, dY \tag{14}$$

Boundary conditions and dimensions are shown in Fig. 1. They can be listed as:

On the moving (top) lid ($0 \leqslant X \leqslant 1, Y = 1$): $U = 1$, $V = 0$ (+x direction), $\frac{\partial\theta}{\partial Y} = 0$; $U = -1$, $V = 0$ ($-x$ direction), $\frac{\partial\theta}{\partial Y} = 0$.
On the right vertical wall ($X = 1, 0 \leqslant Y \leqslant 1$): $U = 0$, $V = 0$, $\theta = 0$.
On the left vertical wall ($X = 0, 0 \leqslant Y \leqslant 1$): $U = 0$, $V = 0$, $\theta = 1$.
On the bottom wall ($0 \leqslant X \leqslant 1, Y = 0$): $U = 0$, $V = 0$, $\frac{\partial\theta}{\partial Y} = 0$.
On the solid (fin)/fluid interface: $\frac{\partial\theta}{\partial X}\big|_s = K\frac{\partial\theta}{\partial X}\big|_f$, $\frac{\partial\theta}{\partial Y}\big|_s = K\frac{\partial\theta}{\partial Y}\big|_f$.

4. Numerical methods

The commercial software Fluent was used for the calculation and Gambit was used for spatial discretization [32]. The SIMPLE method was used to couple the velocity and pressure term [33]. QUICK (Quadratic Upwind Interpolation for Convective Kinematics) scheme [34] was performed for the discretization of convective terms in the momentum and energy equations. Uniform grids were generated. We used four sets of grids, changing from 64×64 to 120×120, to do the calculation for three typical cases to check the effect of grid numbers on the results. After comparison, 100×100 grid dimension is considered enough for calculation.

The present work was compared to Refs. [35–38]. The comparison results are shown in Table 1. It shows that the results are reasonable and reliable using the method in our present work.

In this study, two validation tests were performed to compare obtained results with literature. In the first case, the computational procedure was validated by the numerical results of Iwatsu and Hyun [11] and Sharif [12] for a top heated moving lid and bottom cooled square cavity filled with air (*Pr* = 0.71). The general agreement between the present computation and those of Iwatsu and

Hyun [11] and Sharif [12] are seen to be very well with a maximum difference within 5%. In the second case, we compared our results with Kahveci [39]. In his case, conjugate-natural convection heat transfer and fluid flow was performed for a fully partitioned square enclosure. Both results showed a good agreement between each other.

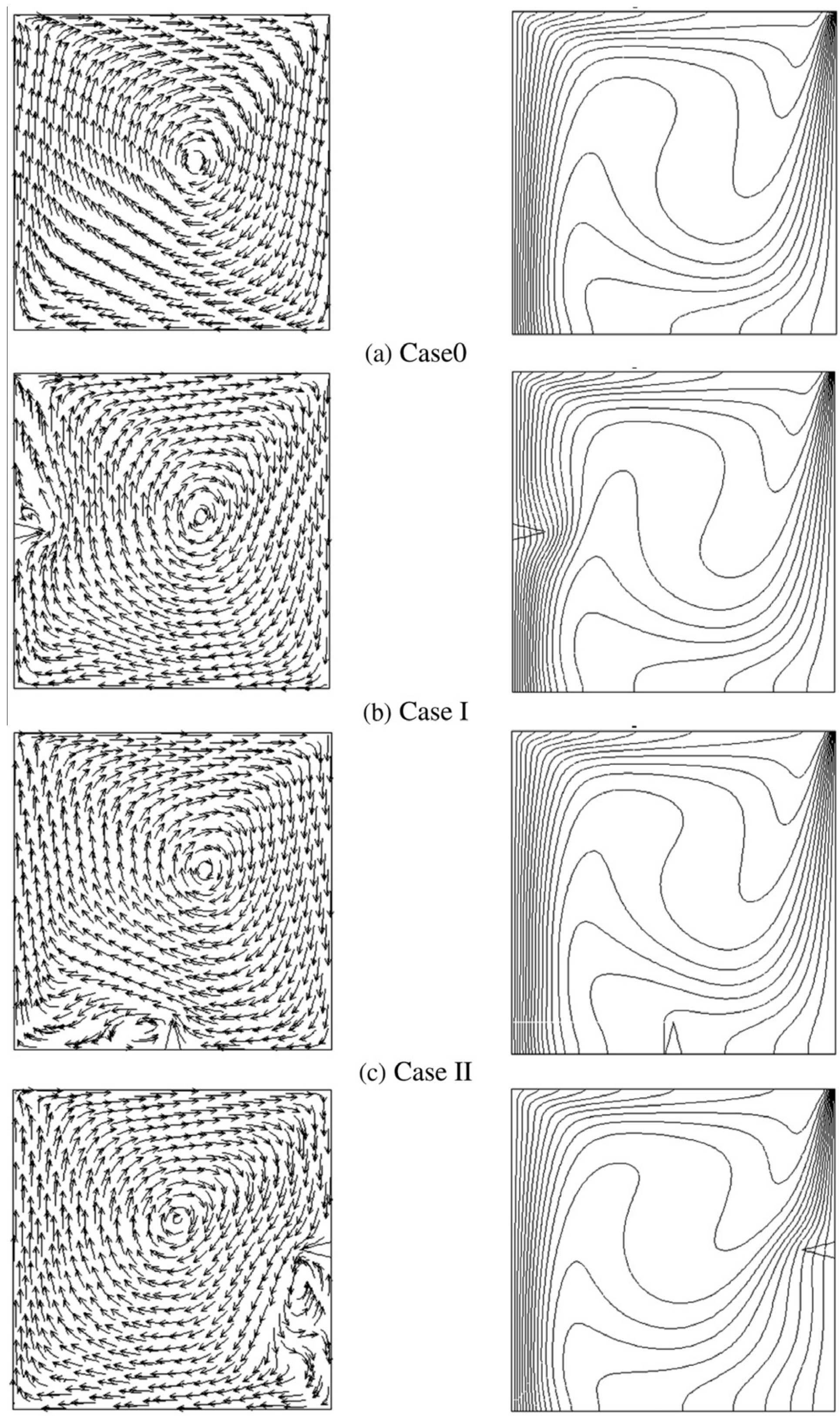

(a) Case0

(b) Case I

(c) Case II

(d) Case III

Fig. 4. Streamlines with arrows and isotherms for different cases with lid moving in the +x direction at Ri = 1.0.

5. Results and discussion

In this study, the fin is located on the center of left wall, right wall and bottom wall in three cases. $Ri = 0.1$, 1.0, 10.0, $K = 0.1$, 1.0, 10.0 and Grashof number is fixed at 10^5. Prandtl number is taken as 0.71 corresponding to air.

Mean Nusselt numbers at different Ri and K are shown in Table 2. They increase with decreasing Ri at the same K indicating that the faster the lid moves the stronger heat transfer. They decrease with increasing K at the same Ri because heat conduction of the fin becomes weak. However, this decrease is very small. The streamlines, isotherms and local Nu at $K = 0.1$, 1.0, 10.0 are almost the same respectively (not shown restricted to page numbers). Thus, the results at $K = 1.0$ is selected for discussions below. The Table 3 presents the effects of lid direction for different cases at different Richardson number. It is shown that direction of lid makes important effect on heat transfer.

When the top lid moves in the +x direction, flow and heat transfer results for three locations of the fin are compared with those without fin. At $Ri = 0.1$ (Fig. 2), the existence of the fin generates a large vortex downstream due to the disturbance of the fin on the flow field. The greatest disturbance is achieved when the fin is on the right wall. When the fin is on the bottom wall, the isotherms do not change much because the bottom wall is adiabatic. When the fin is on the left wall, the interval of the isotherms at the location of the fin becomes larger compared to Case 0. The greatest influence on the isotherms is achieved when the fin is on the right wall corresponding to the location for the greatest disturbance on the flow field. The reason of the widened isotherms is that flow velocity is reduced around the fin so that heat convection is weakened and heat conduction is dominant. Compared with the local Nusselt number on the left wall in Case 0 (Fig. 3(a)), the local Nusselt number on the left wall of Case I is smaller below $Y = 0.8$ and larger above $Y = 0.8$; the local Nusselt number on the left wall of

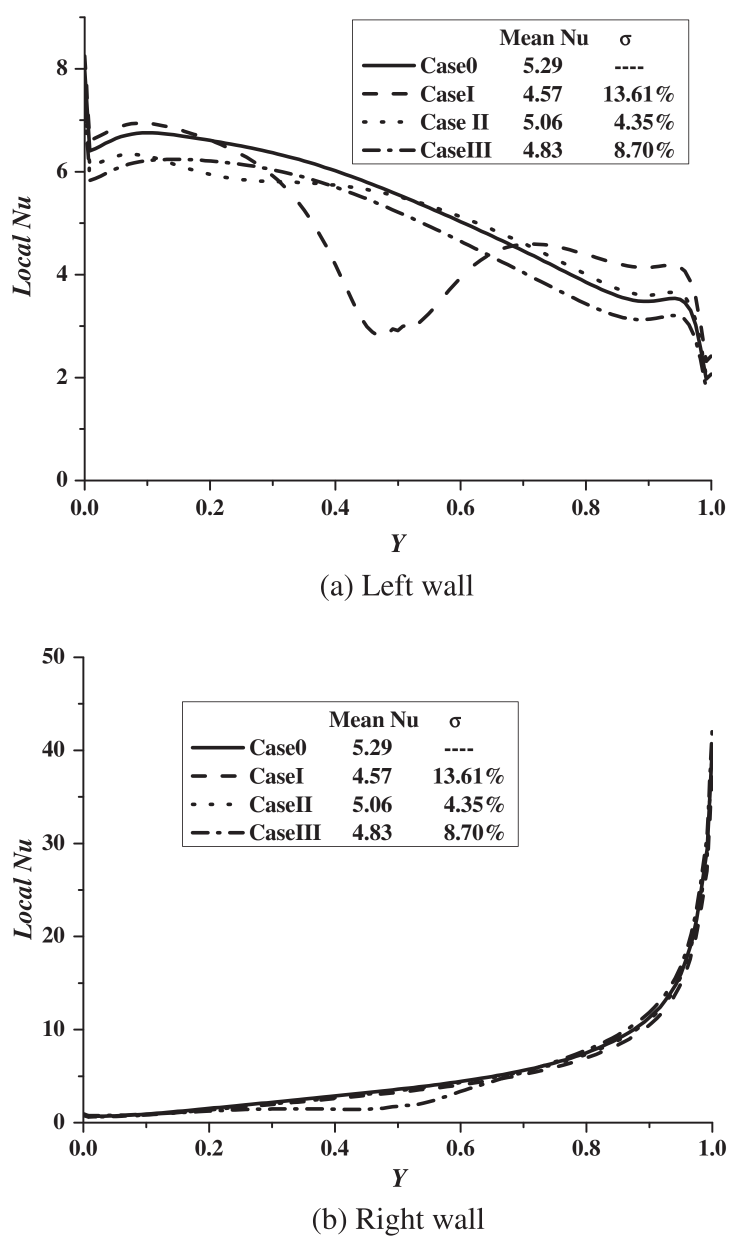

Fig. 5. Local Nusselt number and the mean Nu for different cases with lid moving in the +x direction at $Ri = 1.0$. $^*\sigma = \frac{\overline{Nu}_{\text{Case0}} - \overline{Nu}_{\text{Case}(J)}}{\overline{Nu}_{\text{Case0}}} \times 100\% \quad J = \text{I}, \text{II}, \text{III}$.

Case II is smaller below $Y = 0.4$ and larger above $Y = 0.4$; the local Nusselt number on the left wall of Case III is smaller below $Y = 0.5$ and larger above $Y = 0.5$. The distribution of the local Nusselt number on the right wall (Fig. 3(b)) does not change

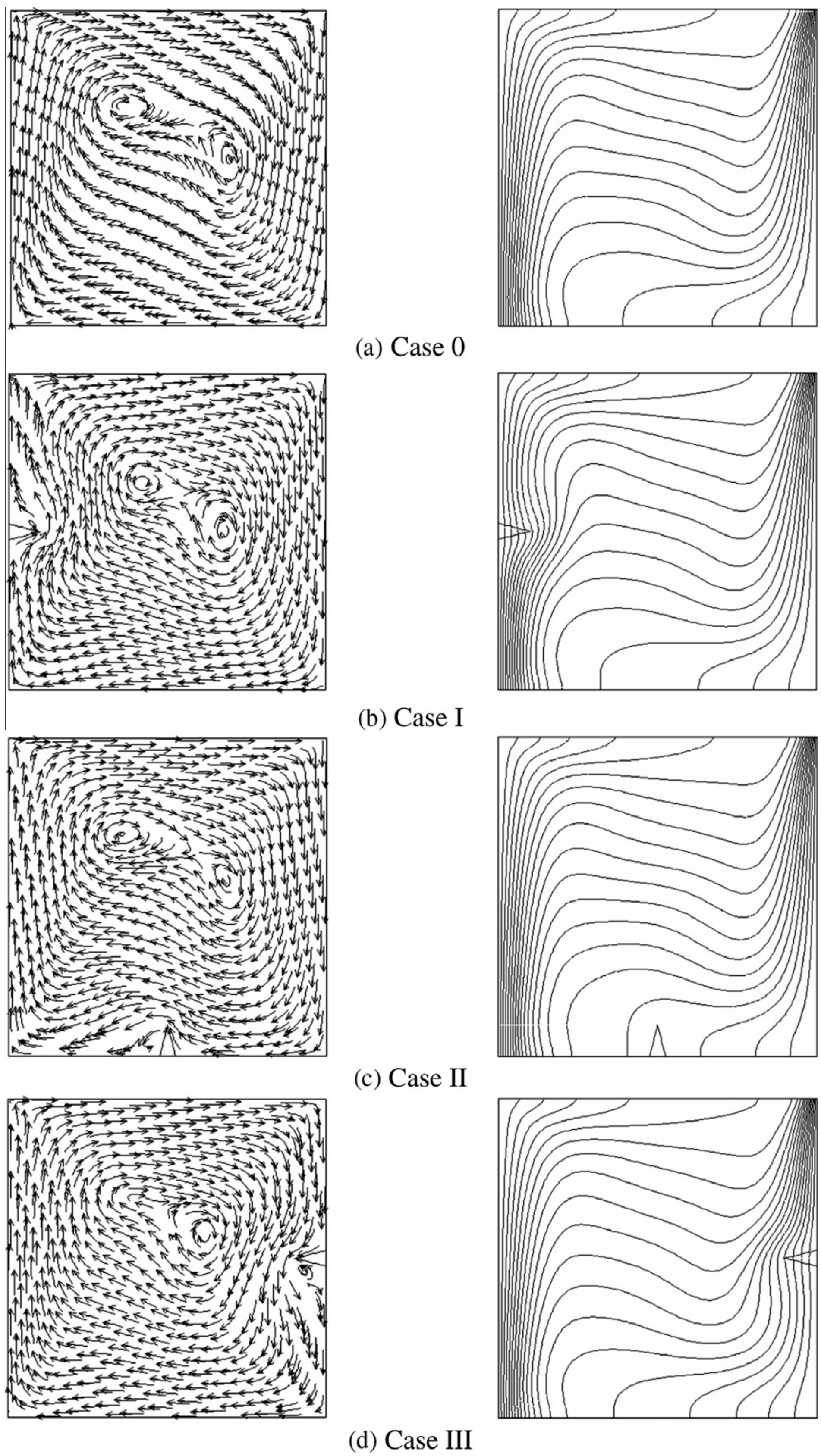

Fig. 6. Streamlines with arrows and isotherms for different cases with lid moving in the $+x$ direction at $Ri = 10.0$.

apparently for Case I and Case II. In Case III, the local Nusselt number on the right wall fluctuates around $Y = 0.4$. The mean Nusselt number decreases by 26.27%, 8.71% and 13.27% for Case I, Case II and Case III, respectively compared to Case 0.

At $Ri = 1.0$ (Fig. 4), the fin only generates a small downstream vortex while the forced convection is comparable with the natural convection. The influences of the left-wall-fin and the right-wall-fin on the isotherms are comparable. Compared with the local Nusselt number on the left wall in Case 0 (Fig. 5(a)), the local Nusselt number on the left wall of Case I is smaller between $Y = 0.2$ and $Y = 0.7$; the local Nusselt number on the left wall of Case II is smaller below $Y = 0.5$ and larger above $Y = 0.5$; the local Nusselt number on the left wall of Case III is smaller along the whole left wall. Compared with the local Nusselt number on the right wall in Case 0 (Fig. 5(b)), the local Nusselt number on the right wall of Case III is smaller between $Y = 0.2$ and $Y = 0.8$ while the local Nusselt numbers on the right wall of the other two cases are almost the same. The mean Nusselt number decreases by 13.61%, 4.35% and 8.70% for Case I, Case II and Case III, respectively compared to Case 0.

At $Ri = 10.0$ (Fig. 6), the influence of the fin on the flow field is slight because the forced convection is weak. Velocities become all clockwise. Correspondingly, the isotherms have tiny changes around the fin. It can be seen in Fig. 7(a) that the comparison results of the local Nusselt number on the left wall are the same as those at $Ri = 1.0$ (Fig. 5(a)). On the right wall (Fig. 7(b)), the local Nusselt number of Case III drops down between $Y = 0.3$ and $Y = 0.7$ while the local Nusselt numbers of the other two cases do not change compared to Case 0. The mean Nusselt number decreases by 10.63%, 2.39% and 9.33% for Case I, Case II and Case III, respectively compared to Case 0.

When the top lid moves in the $-x$ direction, flow and heat transfer results for three locations of the fin are also compared with those without fin. At $Ri = 0.1$ (Fig. 8), the fin on the left wall causes the two corner vortexes to form a large one. The fin on the bottom wall or the right wall makes the two corner vortexes larger. A very small vortex can be found downstream of the fin when the fin is on the right wall. The greatest impact on the isotherms occurs when the fin is on the left wall where the interval of the isotherms is

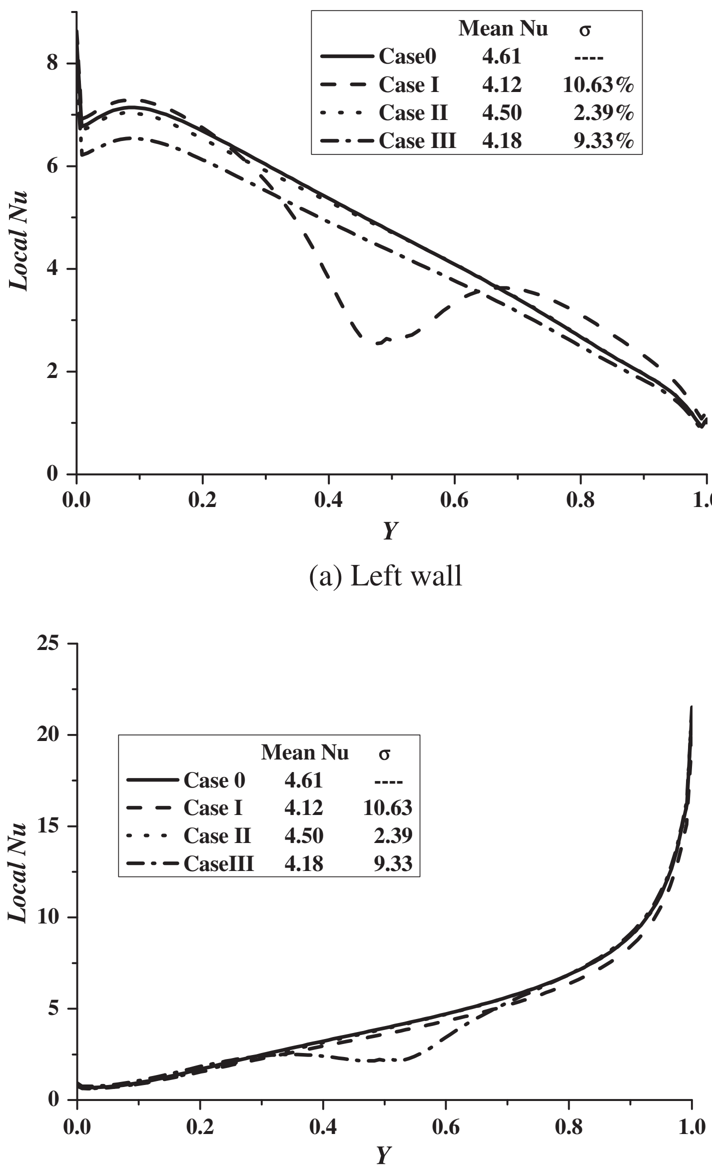

(a) Left wall

(b) Right wall

Fig. 7. Local Nusselt number and the mean Nu for different cases with lid moving in the +x direction at $Ri = 10.0$. $^{*}\sigma = \frac{\overline{Nu}_{\text{Case0}} - \overline{Nu}_{\text{Case}(J)}}{\overline{Nu}_{\text{Case0}}} \times 100\% \quad J = \text{I, II, III}$.

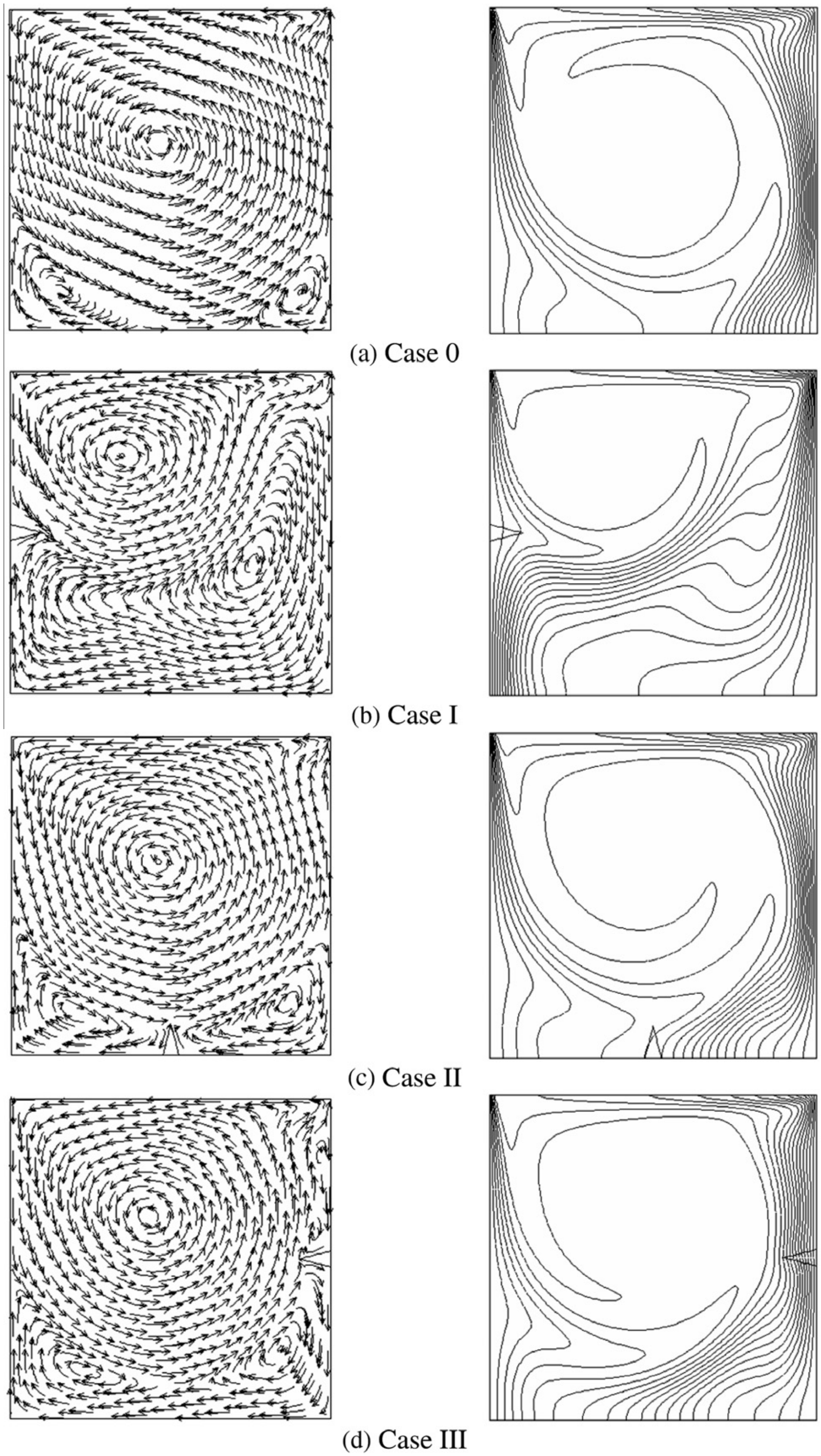

Fig. 8. Streamlines with arrows and isotherms for different cases with lid moving in the $-x$ direction at $Ri = 0.1$.

larger than Case 0, indicating that the temperature gradient is smaller. Compared with the local Nusselt number on the left wall in Case 0 (Fig. 9(a)), the local Nusselt number on the left wall of Case I is smaller below $Y = 0.4$ and larger above $Y = 0.4$; the local Nusselt numbers on the left wall of the other two cases are almost the same. Compared to the local Nusselt number on the right wall

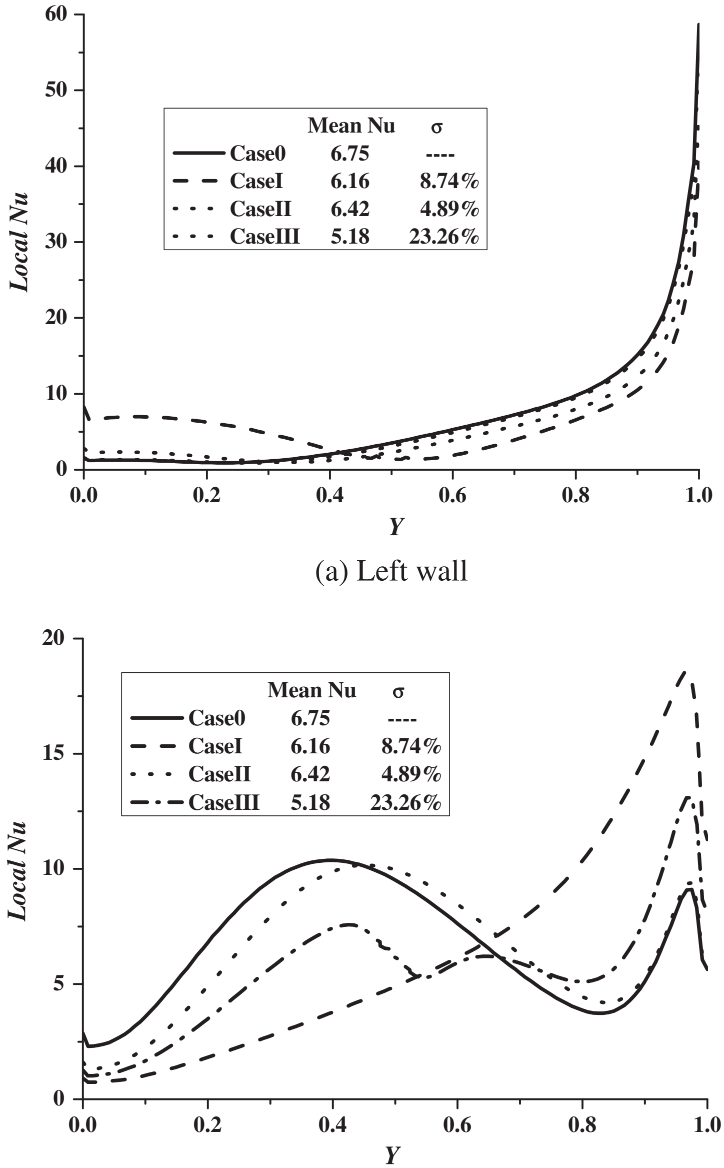

(a) Left wall

(b) Right wall

Fig. 9. Local Nusselt number and the mean *Nu* for different cases with lid moving in the $-x$ direction at *Ri* = 0.1. $^{*}\sigma = \frac{\overline{Nu}_{\text{Case0}} - \overline{Nu}_{\text{Case(J)}}}{\overline{Nu}_{\text{Case0}}} \times 100\% \quad J = \text{I, II, III}$.

in Case 0 (Fig. 9(b)), the local Nusselt number on the right wall of Case I is smaller below $Y = 0.65$ and larger above $Y = 0.65$; the local Nusselt number on the right wall of Case II is smaller below $Y = 0.45$ and larger above $Y = 0.45$; the local Nusselt number on the right wall of Case III is smaller below $Y = 0.7$ and larger above $Y = 0.7$. The mean Nusselt number for three locations decreases by 8.74%, 4.89% and 23.26% for Case I, Case II and Case III, respectively compared to Case 0.

At $Ri = 1.0$ (Fig. 10), the cavity without fin is occupied by two large vortexes. The lower one is clockwise. The upper one is counterclockwise since it is generated by the top lid. When the fin is on the left wall, the interaction of the two vortexes goes down due to the fin locally restricts flow. When the fin is on the bottom wall or the right wall, it only affects the clockwise vortex nearby. The fin does not change the isotherms much even in the local area of the fin, no matter where it is. Compared with the local Nusselt number on the left wall in Case 0 (Fig. 11(a)), the local Nusselt number on the left wall of Case I decreases between $Y = 0.25$ and $Y = 0.65$ while the local Nusselt numbers on the left wall of the other two cases are almost the same. Compared with the local Nusselt number on the right wall in Case 0 (Fig. 11(b)), the local Nusselt number on the right wall of Case I is smaller along the whole right wall; the local Nusselt number on the right wall of Case II does not change apparently; the local Nusselt number on the right wall of Case III is smaller between $Y = 0.35$ and $Y = 0.78$. The mean Nusselt number decreases by 5.19%, 1.8% and 12.57% for three locations, respectively compared to Case 0.

At $Ri = 10.0$ (Fig. 12), the vortex driven by the lid is restricted to the top area since the forced convection is weaker than the natural convection. The fin on the left, bottom or right wall disturbs the flow field only locally. The streamlines are smooth and no vortex generates. Flow field far from the fin is almost not affected by the fin. The impact of the left-wall-fin on the isotherms is comparable with that of the right-wall-fin. The impact of the fin can be neglected when it is on the bottom wall. Compared with the local Nusselt number on the left wall in Case 0 (Fig. 13(a)), the local

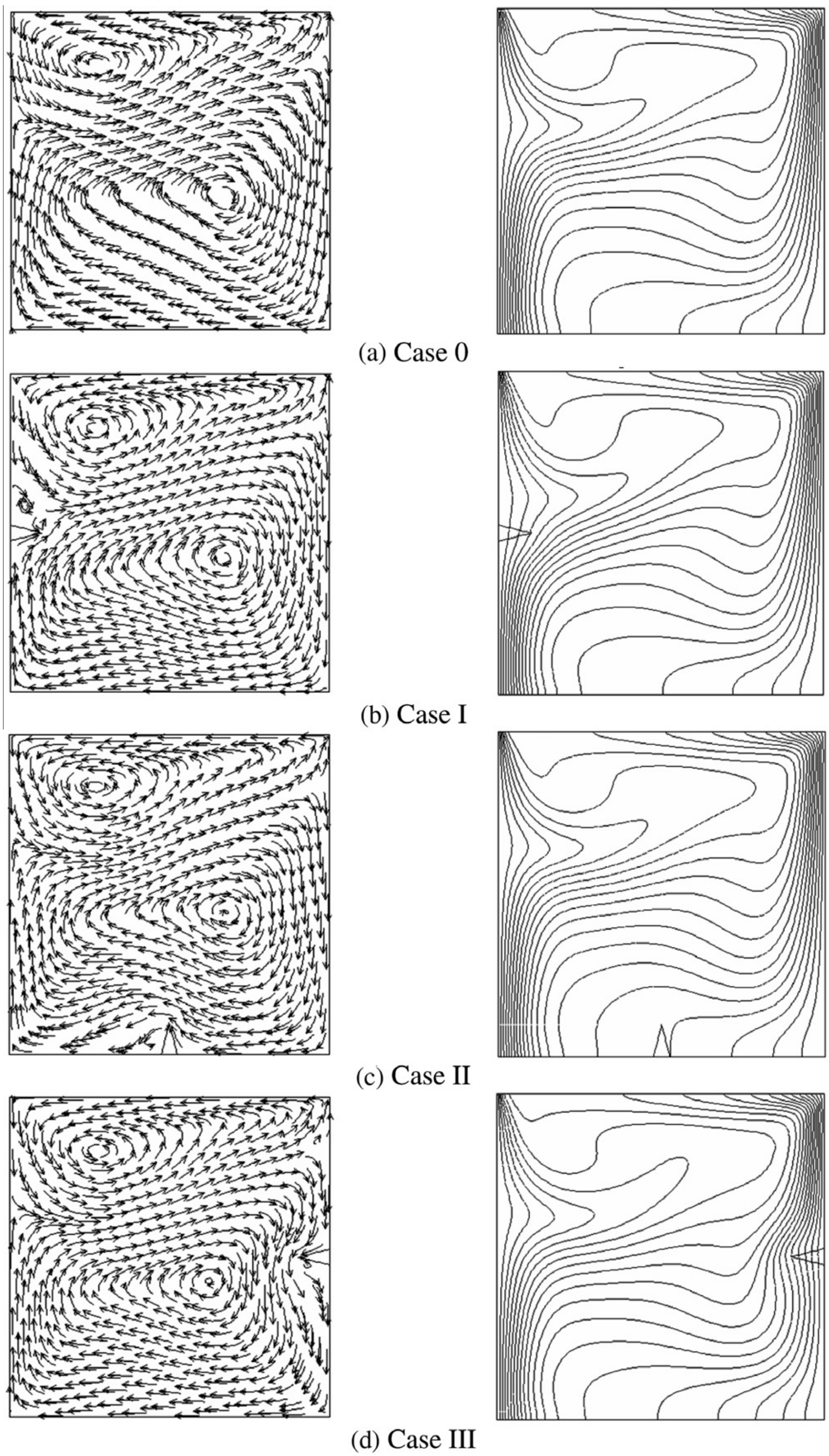

Fig. 10. Streamlines with arrows and isotherms for different cases with lid moving in the $-x$ direction at Ri = 1.0.

Nusselt number on the left wall of Case I is smaller between Y = 0.2 and Y = 0.7; the local Nusselt number on the left wall of Case II does not change much; the local Nusselt number on the left wall of Case III is smaller along the whole left wall. Compared to the local Nusselt number on the right wall in Case 0 (Fig. 13(b)), the local Nusselt number on the right wall of Case I is smaller along the

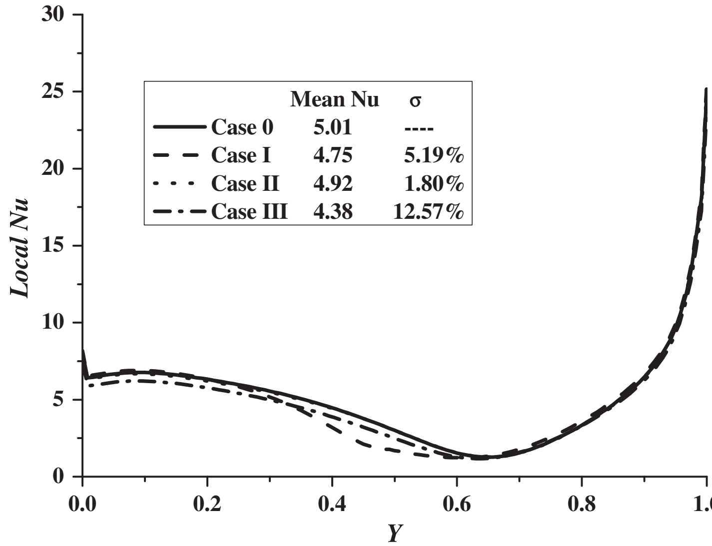

(a) Left wall

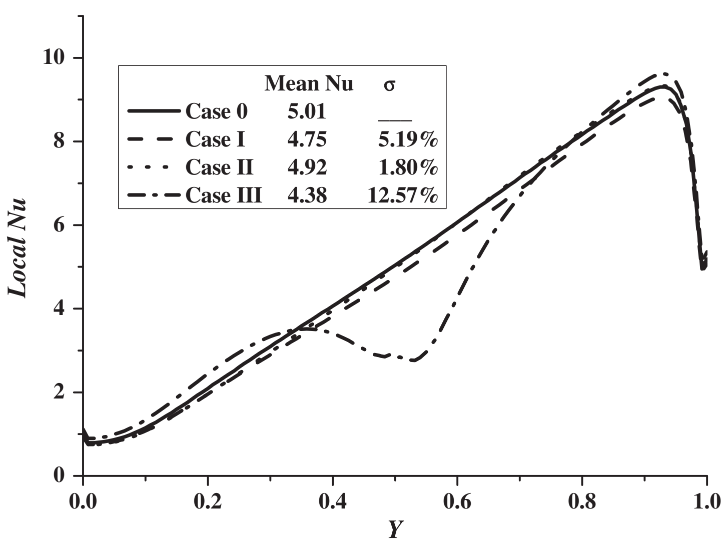

(b) Right wall

Fig. 11. Local Nusselt number and the mean Nu for different cases with lid moving in the $-x$ direction at Ri = 1.0. $^{*}\sigma = \frac{\overline{Nu}_{\text{Case0}} - \overline{Nu}_{\text{Case}(J)}}{\overline{Nu}_{\text{Case0}}} \times 100\% \quad J = \text{I}, \text{II}, \text{III}$.

whole right wall; the local Nusselt number on the right wall of Case II does not change much; the local Nusselt number on the right wall of Case III is smaller between Y = 0.3 and Y = 0.7. The mean Nusselt number decreases by 9.23%, 1.75% and 10.72% for Case I, Case II and Case III, respectively compared to Case 0.

From the analyses above, summarizations can be made as follows. With the lid moving in the +x direction, the fin on the left wall decreases the mean Nusselt number most. When the forced convection is dominant, the fin on the right wall changes the streamlines and isotherms most; when the two convections are comparable, three locations of the fin have the same impact on the streamlines and isotherms; when the natural convection is dominant, the fin has no influence on the streamlines and isotherms no matter where it is. With the lid moving in the $-x$ direction, the fin on the right wall has the greatest impacts on the mean Nusselt number. When the forced convection is dominant, the fin on the left wall changes the streamlines and isotherms most; when the two convections are comparable or the natural convection is dominant, three locations of the fin have the same impact on the streamlines and have no influence on the isotherms no matter where it is.

6. Conclusions

Based on the analyses in Section 5, the conclusions can be made as follows:

(1) The mean Nu decreases with increasing K. Streamlines, isotherms and local Nu change very slightly with K.
(2) The existence of the fin decreases the mean Nu because the fin interrupts the mixed convections. The largest decrease is 26.37% when the fin is on the left wall and Ri = 0.1 with the lid moving in the +x direction.
(3) The fin reduces the fluid velocity nearby causing the weakened heat convection. Thus, the local Nu in this area is smaller than that without fin.

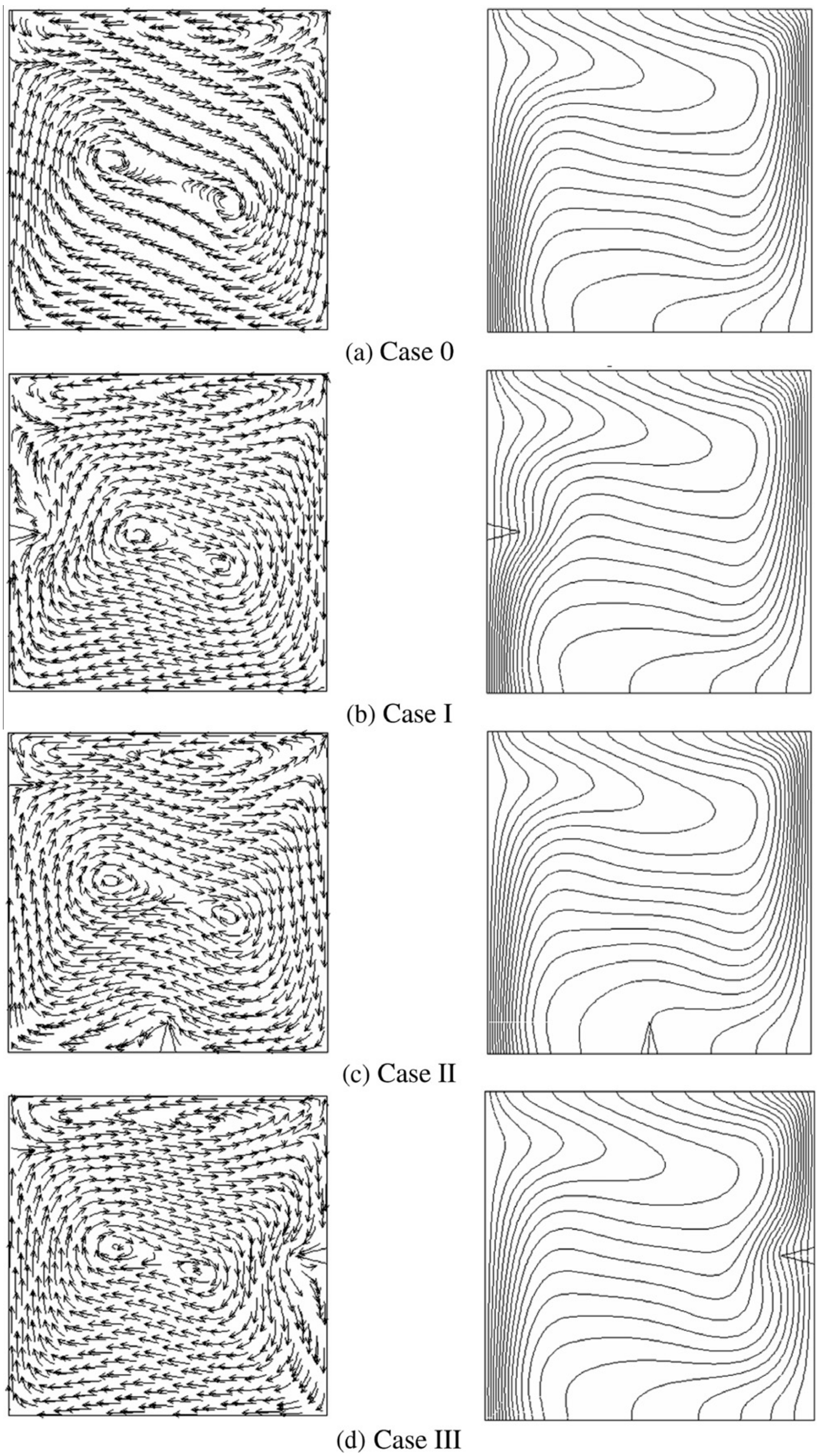

Fig. 12. Streamlines with arrows and isotherms for different cases with lid moving in the $-x$ direction at $Ri = 10.0$.

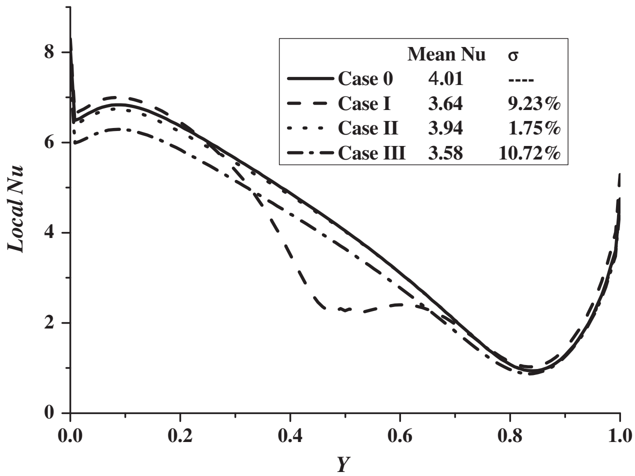

(a) Left wall

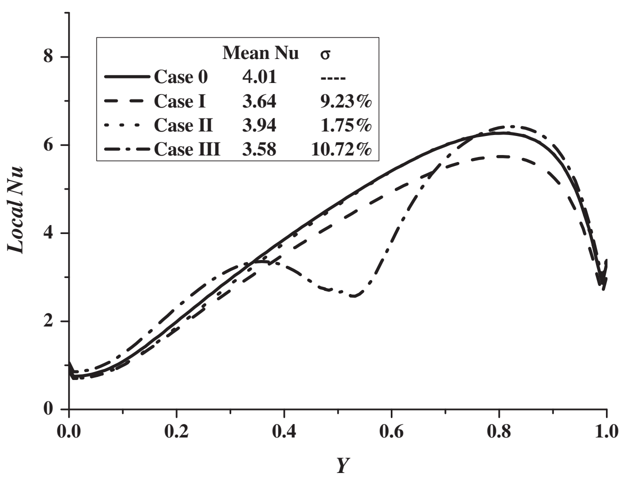

(b) Right wall

Fig. 13. Local Nusselt number and the mean *Nu* for different cases with lid moving in the $-x$ direction at *Ri* = 10.0. $^{*}\sigma = \frac{\overline{Nu}_{\mathrm{Case0}} - \overline{Nu}_{\mathrm{Case}(J)}}{\overline{Nu}_{\mathrm{Case0}}} \times 100\% \quad J = \mathrm{I}, \mathrm{II}, \mathrm{III}.$

(4) The fin on the vertical walls causes the isotherms wider. The fin on the bottom wall has no influence on the isotherms because the bottom wall is adiabatic and the fluid has no heat exchange with the bottom wall.

(5) When the top lid moves in the +*x* direction, the fin has the greatest impact on the flow field when it is attached to the left wall. When the top lid moves in the $-x$ direction, the fin achieves the greatest impact on the flow field when it is attached to the right wall. The fin on the bottom wall has tiny effect on the flow field and isotherms no matter which direction the top lid moves.

Acknowledgements

The study is supported by the National Science Foundation of China (No. 50876114 and No. 10602043); the State Key Laboratory of Multiphase Flow in Power Engineering (Xi'an Jiaotong University); SRF for ROCS, SEM and the New Century Excellent Talents in Ministry of Education Support Program (NCET-07-0843, NCET-07-0680).

References

[1] C.K. Cha, Y. Jaluria, Recirculating mixed convection flow for energy extraction, Int. J. Heat Mass Transfer 27 (1984) 1801–1810.
[2] J. Imberger, P.F. Hamblin, Dynamics of lake reservoirs and cooling ponds, Annu. Rev. Fluid Mech. 14 (1982) 153–187.
[3] P.N. Shankar, M.D. Deshpande, Fluid mechanics in the driven cavity, Annu. Rev. Fluid Mech. 32 (2000) 93–136.
[4] U. Ghia, K.N. Ghia, C.T. Shin, High-Re solutions for incompressible flow using the Navier–Stokes equations and a multigrid method, J. Comput. Phys. 48 (1982) 387–411.
[5] R. Schreiber, H.B. Keller, Driven cavity flows by efficient numerical techniques, J. Comput. Phys. 49 (1983) 310–333.
[6] M.C. Thompson, J.H. Ferziger, An adaptive multigrid technique for the incompressible Navier–Stokes equations, J. Comput. Phys. 82 (1989) 94–121.
[7] D.L. Young, J.A. Liggett, R.H. Gallagher, Unsteady stratified circulation in a cavity, ASCE J. Eng. Mech. Div. 102 (EM6) (1976) 1009–1023.
[8] A.J. Chamkha, Hydromagnetic combined convection flow in a vertical lid-driven cavity with internal heat generation or absorption, Numer. Heat Transfer, Part A 41 (2002) 529–546.
[9] O. Aydin, Aiding and opposing mechanisms of mixed convection in a shear- and buoyancy-driven cavity, Int. Commun. Heat Mass Transfer 26 (1999) 1019–1028.
[10] C.J. Freitas, R.L. Street, A.N. Findikakis, J.R. Koseff, Numerical Simulation of three-dimensional flow in a cavity, Int. J. Numer. Methods Fluids 5 (1985) 561–575.
[11] R. Iwatsu, J.M. Hyun, Three-dimensional driven-cavity flows with a vertical temperature gradient, Int. J. Heat Mass Transfer 38 (1995) 3319–3328.
[12] M.A.R. Sharif, Laminar mixed convection in shallow inclined driven cavities with hot moving lid on top and cooled from bottom, Appl. Therm. Eng. 27 (2007) 1036–1042.
[13] M. Morzynski, Cz.O. Popiel, Laminar heat transfer in a two-dimensional cavity covered by a moving wall, Numer. Heat Transfer 13 (1988) 265–273.
[14] C.J. Freitas, R.L. Street, Non-linear transport phenomena in a complex recirculation flow: a numerical investigation, Int. J. Numer. Methods Fluids 8 (1988) 769–802.
[15] R. Iwatsu, J.M. Hyun, K. Kuwahara, Convection in a differentially-heated square cavity with a torsionally-oscillating lid, Int. J. Heat Mass Transfer 35 (1992) 1069–1076.
[16] A.A. Mohamad, R. Viskanta, Stability of lid-driven shallow cavity heated from below, Int. J. Heat Mass Transfer 32 (1989) 2155–2166.
[17] H.F. Oztop, I. Dagtekin, Mixed convection in two-sided lid-driven differentially heated square cavity, Int. J. Heat Mass Transfer 47 (2004) 1761–1769.
[18] N. Alleborn, H. Raszillier, F. Durst, Lid-driven cavity with heat and mass transport, Int. J. Heat Mass Transfer 42 (1999) 833–853.
[19] X. Shi, J.M. Khodadadi, Fluid flow and heat transfer in a lid-driven cavity due to an oscillating thin fin: transient behavior, J. Heat Transfer 126 (2004) 924–930.
[20] X. Shi, J.M. Khodadadi, Laminar fluid flow and heat transfer in a lid-driven cavity due to a thin fin, J. Heat Transfer 124 (2002) 1056–1063.
[21] X. Shi, J.M. Khodadadi, Fluid flow and heat transfer in a lid-driven cavity due to an oscillatory thin fin: transient behavior, in: Proceedings of HT/FED 2004: Heat Transfer/Fluids Engineering Summer Conference, July 11–15, 2004, Charlotte, North Carolina, pp. 1–9.
[22] H.F. Oztop, Laminar fluid flow and heat transfer in a lid-driven cavity with rectangular body inserted, in: 14th Conference on Thermal Engineering and Thermogrammetry, Budapest, Hungary, 2005.
[23] I. Dagtekin, H.F. Oztop, Mixed convection in an enclosure with a vertical heated block located, in: Proceedings of ESDA2002: 6th Biennial Conference on Engineering Systems Design and Analysis, Istanbul, Turkey.
[24] S.K. Mahapatra, A. Sarkar, A. Sarkar, Numerical simulation of opposing mixed convection in differentially heated square enclosure with partition, Int. J. Therm. Sci. 46 (2007) 970–979.
[25] D. Mansutti, G. Graziani, R. Piva, A discrete vector potential model for unsteady incompressible viscous flows, J. Comput. Phys. 92 (1991) 161–184.
[26] G. Ruocco, Entropy generation in conjugate heat transfer from a discretely heated plate to an impinging confined jet, Int. Commun. Heat Mass Transfer 24 (1997) 201–210.
[27] F. Sarghini, G. Ruocco, Enhancement and reversal heat transfer by competing modes in jet impingement, Int. J. Heat Mass Transfer 47 (2004) 1711–1718.
[28] B. Premachandran, C. Balaji, Conjugate mixed convection with surface radiation from a horizontal channel with protruding heat sources, Int. J. Heat Mass Transfer 49 (2006) 3568–3582.
[29] H.F. Oztop, C. Sun, B. Yu, Conjugate-mixed convection heat transfer in a lid-driven enclosure with thick bottom wall, Int. Commun. Heat Mass Transfer 35 (2008) 779–785.
[30] H.F. Oztop, Z. Zhao, B. Yu, Fluid flow due to combined convection in lid-driven enclosure having a circular body, Int. J. Heat Fluid Flow 30 (2009) 886–901.
[31] T. Basak, S. Roy, P.K. Sharma, I. Pop, Analysis of mixed convection flows within a square cavity with uniform and non-uniform heating of bottom wall, Int. J. Therm. Sci. 48 (2009) 891–912.

[32] T. Basak, S. Roy, P.K. Sharma, I. Pop, Analysis of mixed convection flows within a square cavity with linearly heated side wall(s), Int. J. Heat Mass Transfer 52 (2009) 2224–2242.
[33] T. Basak, S. Roy, S.K. Singh, I. Pop, Analysis of mixed convection in a lid-driven porous square cavity with linearly heated side wall(s), Int. J. Heat Mass Transfer 53 (2010) 1819–1840.
[34] FLUENT User's Guide, Fluent Inc., 2002.
[35] G. Barakos, E. Mitsoulis, D. Assimacopoulds, Natural convection flow in a square cavity revisited: laminar and turbulent models with wall functions, Int. J. Numer. Methods Fluids 18 (1994) 695–719.
[36] N.C. Markatos, K.A. Pericleous, 'Laminar and turbulent natural convection in an enclosed cavity, Int. J. Heat Mass Transfer 27 (1984) 755–772.
[37] G. De Vahl Davis, Natural convection of air in a square cavity, a bench-mark numerical solution, Int. J. Numer. Methods Fluids 3 (1983) 249–264.
[38] T. Fusegi, J.M. Hyun, K. Kuwahara, B. Farouk, A numerical study of three-dimensional natural convection in a differentially heated cubical enclosure, Int. J. Heat Mass Transfer 34 (1991) 1543–1577.
[39] K. Kahveci, A differential quadrature solution of natural convection in an enclosure with a finite thickness partition, Numer. Heat Transfer, Part A 51 (2007) 979–1002.